A Study of a Silicon Quasi-Periodic Segmented Waveguide

Marcos Túlio Antunes Bezerra Segundo[1], José Patrocínio da Silva[1]
[1]*Department of Electrical Engineering, Federal University of Rio Grande do Norte, Natal, Brazil,*
marcos.segundo.092@ufrn.edu.br, patroc@ct.ufrn.br

Abstract— **This paper presents a study of a segmented waveguide where the layers are distributed following the Fibonacci sequence and aims to diminish the scattering losses usually caused by imperfections in the core boundaries of the waveguide. This phenomenon normally happens in structures which present a high contrast between the refractive index of the core and the refractive index of the clad. The analyses were obtained through observations of wave fields that propagates along the waveguide, how the effective refractive index (n_{eff}) varies along the z-direction and the study of its normalized power. The simulation of this photonic component was accomplished with the help of the Vectorial Beam Propagation Method (VBPM).**

Index Terms— Segmented Waveguide; Fibonacci Sequence; Optical Waveguide; VBPM.

I. INTRODUCTION

Optical waveguide works confining the light through a contrast between the refractive index (n) of the core and the clad of the structure, where first has a n higher than its clad. When there is a high contrast in a continuous waveguide, it usually occurs scattering in the core-cladding boundary imperfections [1].

Over time, several methods of reducing these losses have been developed. One of the ways found to avoid scattering losses was try not to use waveguides with square core sections, thus having the width of the base larger than the side walls, but this resulted in only good effects for the Transverse Electrical (TE) mode, practically canceling the Transverse Magnetic configurations (TM) [2]–[4].

Another structure also used is the *photonic crystal*, but this structure model usually presents a photon bandgap interval in the operating frequency [5]. Another problem associated with photonic crystals is their high losses when curved [6], greatly limiting their use in some systems.

With time was developed a new type of dielectric waveguide, the *segmented waveguide*. This structure presents an alternation of the material of its core, where the two material have different refractive index, as shown in Figure 1. Normally $n_1 > n_2$ and n_2 is equal or higher than the refractive index of the clad.

Some applications of the segmented waveguides are to diminish the scattering [2], frequency filters [7], frequency demultiplexer [8], polarization filter and in second harmonic generation [9].

From the study related to the segmentation of the cores of the optical guides, a new type of guide, the subwavelength grating waveguide (SWG), was presented in [2], where its segmentation tries to introduce a grid step smaller than the Bragg condition, which enables the dispersion to decrease and the nucleus to behave as if it were continuous [10]. The SWG exhibits a mode delocalization from
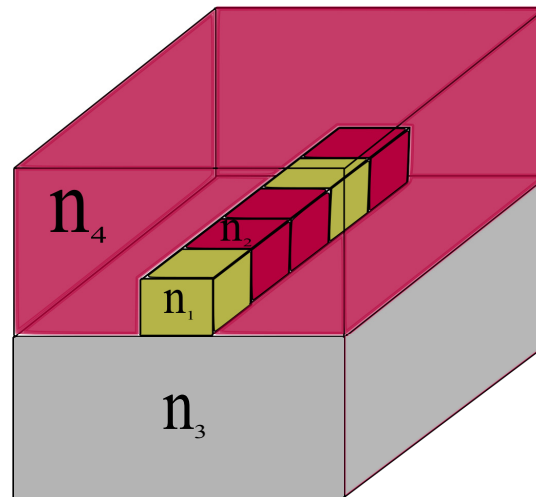
Fig. 1. Example of a segmented waveguide proposed in this work.

the core, which leads to less scattering loss in the boundary between the clad and the core, as well as allowing the control of the effective refractive index without the need to add other materials [10].

Since it was presented the SWG, its characteristics have been highly used in applications as broadband directional couplers [11], multi-mode interference (MMI) couplers [12], fiber-chip couplers [4], [13]–[17], mode-division multiplexers [18], wavelength-division multiplexers [4], evanescent field sensors [19], [20], polarization mode splitters [21]–[23], optical delay lines [24], suspended membrane waveguides for mid-infrared approach [25] and spectral filters based on Bragg gratings [26].

This work presents a new waveguide configuration, based on the SWG model, in which it has a quasi-periodic grid, in this case following the Fibonacci sequence. For the realization of the simulations carried out in this work, it was used the Vectorial Beam Propagation Method (VBPM) [27]. It is important to highlight that this is the first time that this numerical method is used to simulate and analyze this type of segmented waveguide.

This work is organized in the following way: in Section II is presented the VBPM mathematical modeling and the project of the proposed waveguide with its parameters; the results are showed in Section III; and finally in Section IV are presented the conclusions.

II. METHOD ANALYSIS

A. Vectorial Beam Propagation Method (VBPM)

The VBPM is a numerical method that aggregates the Finite Element Method (FEM) with the Beam Propagation Method (BPM) by performing a vector analysis of the fields, making use of the first-order Padé approximation [28], and the use of perfectly matched layers (PML) to avoid undesirable reflections. Its formulation is achieved by first combining Maxwell's equations to obtain (1), which is known as the Helmholtz equation.

$$\nabla \times (\bar{\bar{k}} \nabla \times \vec{H}) - k_0{}^2 \vec{H} = 0 \tag{1}$$

In (1), k_0 is the wave number in free space and $\bar{\bar{k}} = 1/\bar{\bar{\varepsilon}}$, with $\bar{\bar{\varepsilon}}$ being the relative permittivity and,

considering the dielectric materials with transverse anisotropy, is represented as follows:

$$\bar{\bar{\varepsilon}} = \bar{\bar{\varepsilon}}_T + \varepsilon_{zz}\hat{u}_z\hat{u}_z \tag{2}$$

where $\bar{\bar{\varepsilon}}_T$ represents an arbitrary transverse tensor, and $\hat{u}_z$ is associated to the direction z.

Another important information is that the ∇ operator is defined as:

$$\nabla = \hat{u}_x\alpha_x\frac{\partial}{\partial x} + \hat{u}_y\alpha_y\frac{\partial}{\partial y} + \hat{u}_z\alpha_z\frac{\partial}{\partial z} = \nabla_T + \hat{u}_z\alpha_z\frac{\partial}{\partial z} \tag{3}$$

where α_x, α_y and α_z are the parameters relative to the PMLs, and are calculated based on the works [29] and [30].

After some algebraic manipulations, and considering that the field varies slowly with each step in the z-direction [27], we develop the Helmholtz equation, using the Garlekin method [28], to arrive at (4):

$$\begin{aligned}
&\int_\Omega (\bar{\bar{k}}_a\frac{\partial^2\vec{h}_T}{\partial z^2})\cdot\vec{\omega}_T\mathrm{d}\Omega - \int_\Omega (2\gamma\bar{\bar{k}}_a\frac{\partial\vec{h}_T}{\partial z})\cdot\vec{\omega}_T\mathrm{d}\Omega \\
&\quad -\int_{\partial\Omega}(\nabla_T\cdot\vec{h}_T)(\bar{\bar{k}}_b\vec{\omega}_T)\cdot\vec{n}\mathrm{d}l \\
&\quad +\int_\Omega(\nabla_T\cdot\vec{h}_T)\nabla_T(\bar{\bar{k}}_b^{\,T}\vec{\omega}_T)\mathrm{d}\Omega \\
&\quad -\int_{\partial\Omega}(k_{zz}\nabla_T\times\vec{h}_T)\cdot(\vec{\omega}_T\times\vec{n})\mathrm{d}l \\
&\quad -\int_\Omega(k_{zz}\nabla_T\times\vec{h}_T)\cdot(\nabla_T\times\vec{\omega}_T)\mathrm{d}\Omega \\
&\quad +\int_\Omega((\bar{\bar{k}}_c+\gamma\bar{\bar{k}}_a)\vec{h}_T)\cdot\vec{\omega}_T\mathrm{d}\Omega = 0
\end{aligned} \tag{4}$$

where Ω is the domain, $\partial\Omega$ includes all the interfaces and external contours, and the tensors can be defined as:

$$\bar{\bar{k}}_a = \begin{bmatrix} k_{yy} & -k_{yx} \\ -k_{xy} & k_{xx} \end{bmatrix} \tag{5a}$$

$$\bar{\bar{k}}_b = \gamma^{-1}\frac{\partial\bar{\bar{k}}_a}{\partial z} - \bar{\bar{k}}_a \tag{5b}$$

$$\bar{\bar{k}}_c = k_0^2 - \gamma^{-1}\frac{\partial\bar{\bar{k}}_a}{\partial z} \tag{5c}$$

Discretizing (4) using the finite element method, introducing the PMLs parameters directly in the formulation through operator ∇_T, as shown in (3), we achieve the equation (6):

$$[M]\frac{\partial^2\{\vec{h}_T\}}{\partial z^2} - 2\gamma[M]\frac{\partial\{\vec{h}_T\}}{\partial z} + ([K]+\gamma^2[M])\{\vec{h}_T\} = \{0\} \tag{6}$$

where $\{\vec{h}_T\}$ represents a column vector containing unknown values of h_{xj} and h_{yj}, 0 is a null column vector, and $[M]$ and $[K]$ are called global matrices defined in [27].

The next step of the formulation is the application of the non-paraxial approximation of the padé type of order (1,1) [28] in (6), producing the matrix (7):

$$[\tilde{M}]\frac{d\{\vec{h}_T\}}{dz} + [K]\{\vec{h}_T\} = \{0\} \tag{7}$$

where $[\tilde{M}] = [M] - \frac{1}{4\gamma^2}([K] + \gamma^2[M])$.

Finally, if we apply the θ-finite-difference marching scheme in equation (7), we obtain the equation (8) as follows:

$$([\tilde{M}(z)] + \theta\Delta z[K(z)])\{\vec{h}_T(z + \Delta z)\}$$
$$= ([\tilde{M}(z)] - (1-\theta)\Delta z[K(z)])\{\vec{h}_T(z)\} \tag{8}$$

where Δz is the propagation step along the z-direction and $\theta(0 \leq \theta \leq 1)$ is introduced to control the stability of the method. When $\theta = 0.5$, we have a correspondent Crank-Nicholson algorithm [27].

Since the material of waveguide adopt in this paper change along the z-direction, the effective refractive index was calculated in every propagation step (Δz), using the (9):

$$n^2{}_{eff}(z) = Re\left[\frac{\{\vec{h}_T(z)\}^\dagger[K(z)]\{\vec{h}_T(z)\}}{k_0{}^2\{\vec{h}_T(z)\}^\dagger[M(z)]\{\vec{h}_T(z)\}}\right] \tag{9}$$

where $\dagger$ represents the conjugated and transposed complex.

B. Quasi-Periodic Segmented Waveguide

For this work it was proposed a silicon waveguide, where the substrate is silica (SiO_2) and the upper cladding is SU-8 polymer. This waveguide is based on the one proposed in [2], but instead of the use of a periodic segmentation, it is proposed a quasi-periodic segmentation, in this case using the Fibonacci sequence. The Fig. 2 shows the transversal model of the waveguide.
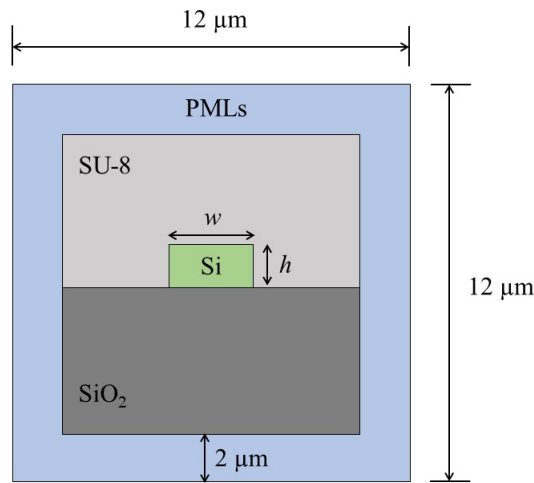

Fig. 2. Used model of the Silicon waveguide

The waveguide structure is based on a sequence of blocks, where the first two blocks of the sequence are A and B, and the next blocks are formed by a superposition of A and B following a rule inspired by the Fibonacci sequence, so that the nth generation of its sequence is obtained by (10).

$$S_n = S_{n-1}S_{n-2} \tag{10}$$

For the (10) $n > 2$, besides $S_1 = A$ and $S_2 = B$. The following are the first generations of the Fibonacci sequence:

$$S_1 = [A], \; S_2 = [B], \; S_3 = [BA], \; S_4 = [BAB], \; etc. \tag{11}$$

For the calculation of each width of the layers, the theory shown in [2], in which the authors claim to have achieved better propagation results for periods of less than half the effective wavelength, was take into account. Based on this work, it was developed calculations of the width of the A with B together, as shown in (12).

$$L_{AB} < \frac{\lambda}{2n_{eff}} \tag{12}$$

Next, it was calculated the separated width of the layers A and B with the help of (13) and (14).

$$L_A = L_{AB}\frac{C_B}{C_T} \tag{13}$$

$$L_B = L_{AB}\frac{C_A}{C_T} \tag{14}$$

Where L_A and L_B are the width of the layers A and B, C_A and C_B are the number of layers A and B for the number of the chosen generation of the Fibonacci sequence, and C_T is the total number of layers. The proportion used in (13) and (14) were adopted after several tests.

The model used was based on the schematic of Fig. 3, in which A and B are the layers of the core that will follow the Fibonacci sequence.
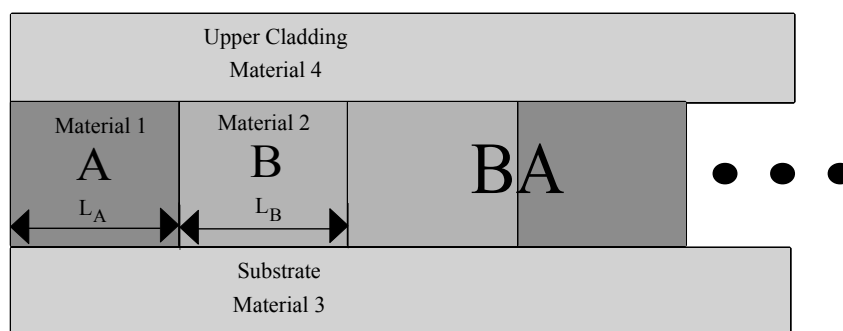

Fig. 3. Model of the Quasi-Periodic Waveguide.

The parameters for this simulation are presented in the Table I. In addition, it was used 2380 finite elements and a propagation step of $0.01\mu m$, during a length of $0.39\mu m$.

TABLE I. **Parameters of the model to be analyzed.**

Material 1	$Si \; (n = 3.476)$
Material 2	$SU-8 \; (n = 1.577)$
Material 3	$SiO_2 \; (n = 1.444)$
Material 4	$SU-8 \; (n = 1.577)$
$L_A(\mu m)$	0.0654
$L_B(\mu m)$	0.0491
$w(\mu m)$	2.000
$h(\mu m)$	1.000
Type of the Waveguide	Rectangular

All simulations were developed in program language FORTRAN, and the graphs were plotted with the help of PYTHON program language.

III. NUMERICAL RESULTS

For this segmented waveguide, it was used the fourth generation of the Fibonacci sequence, which means that it will have seven layers. It was chosen this generation because it was already possible to see the wanted effect in the model of the fields of the wave.

The structure was excited with the fundamental mode obtained from modal analyses, considering several wavelengths and different layers of refractive index, distributed according to the Fibonacci sequence and quasi-periodic in the propagation direction.

In the Fig. 4, it is presented the distribution of the magnetic field when $z = 0\mu m$, while in Fig. 5 it is shown the distribution of the magnetic field in the final stage of the simulation ($z = 0.39\mu m$).
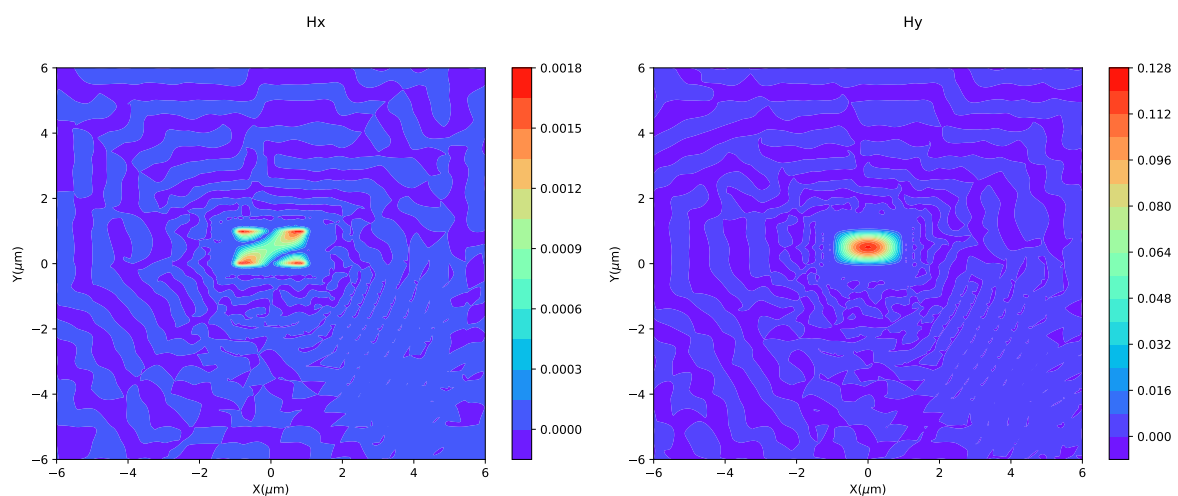

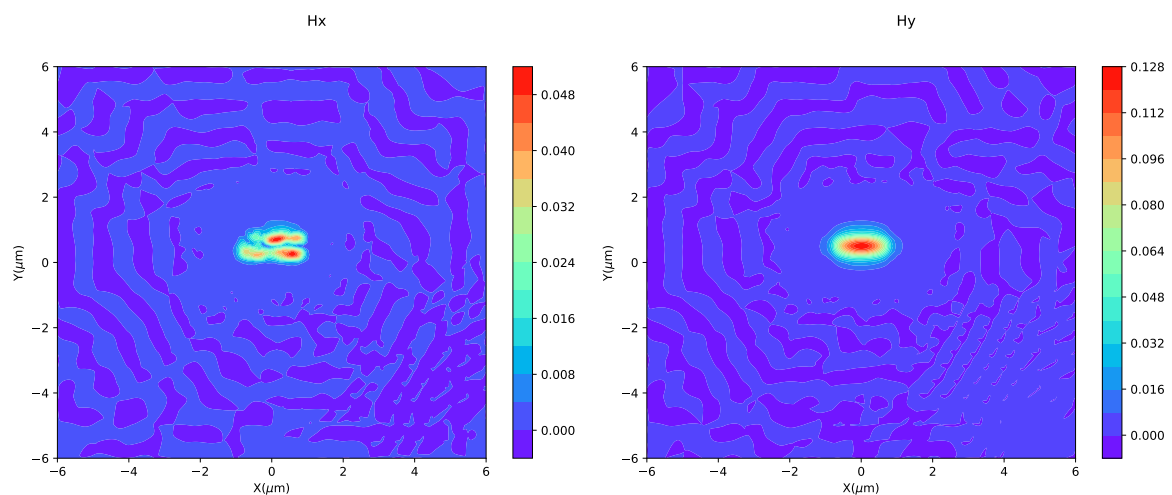Fig. 4. Mode distribution of the field in the beginning of the waveguide.

Fig. 5. Mode distribution of the field in the end of the waveguide.

It is possible to observe in Fig. 5, that the field expands, concentrating less power in the core interface with the clad, reducing the loss for scattering in this region of the waveguide.

Other important propriety that can be observed in the analyses of the results, is that in theses types of waveguides, the effective refraction index (n_{eff}) tends to decrease as propagation occurs, similar of what happens in the periodic SWG. This can be attributed to the small, but existing, insertion losses that occur along the z-direction, due to constant changes in the refractive index of the layers that form the core. The Fig. 6 shows the evolution of the effective refractive index of the quasi-periodic SWG in comparison with the periodic one.
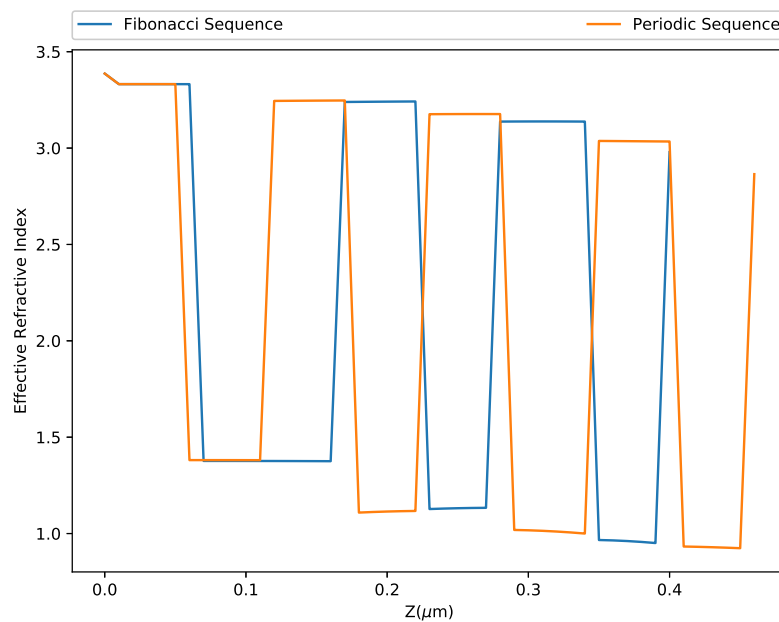

Fig. 6. Effective refractive index along the z-direction.

Since the proposed grid is still smaller than the Bragg grating, the segmented waveguide will have a behavior similar of a continuous waveguide. The Fig. 7 shows the constancy of the component H_y of the magnetic field propagating along the guide.

Comparing the loss of a wave at $\lambda = 1.55 \mu m$, along the waveguide, of the proposed segmented device with the periodic SWG, it can be observed in the Fig. 8 that power of the quasi-periodic waveguide decreases less than last one.
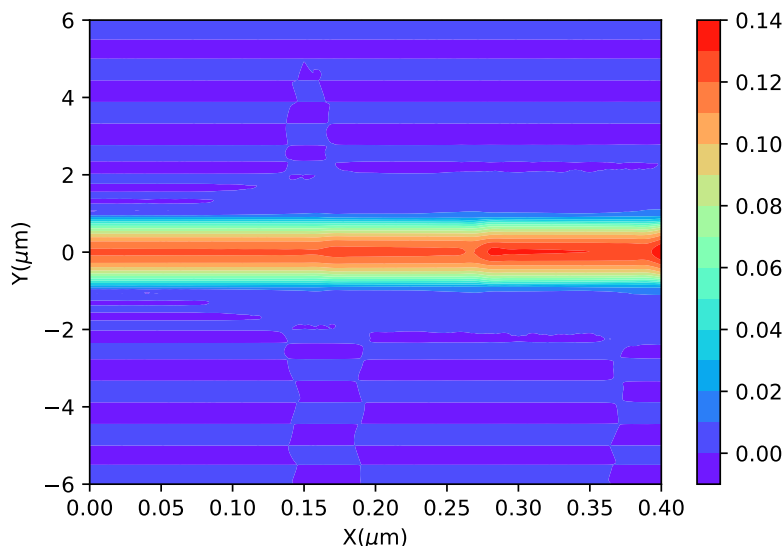
Fig. 7. H_y component of the propagating mode for $y = 0, 5\mu m$ of the proposed waveguide.
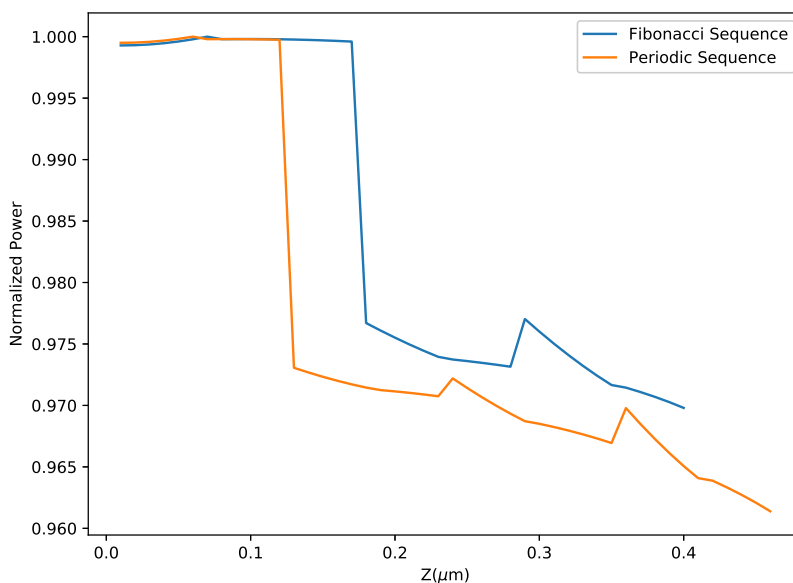

Fig. 8. Comparison of the H_y component normalized power of the quasi-periodic waveguide and the periodic SWG.

Comparing the Fig. 6 with the Fig. 8, it can be noticed that the power along the quasi-periodic waveguide maintain higher than the SWG, because the length that the higher effective index occurs in the proposed device is longer than the usual segmented waveguide. This was already intended when the equations (13) and (14) were developed.

Since the quasi-periodic waveguide will perpetuate this structural characteristic along its longitudinal extension, it can be affirmed that the power behaviour of the device will continue the same along its all length. Adding that the field of the mode was already expanded in this propagation period, as it shown in Fig. 5, it does not display the need of a longer propagation length.

The Fig. 9 shows the normalized power for different wavelengths for the proposed SWG. It can

be observed that the smaller the wavelength, greater it will be the losses. This happens because the frequency of the transmitted wave is getting closer to the band gap of the waveguide.
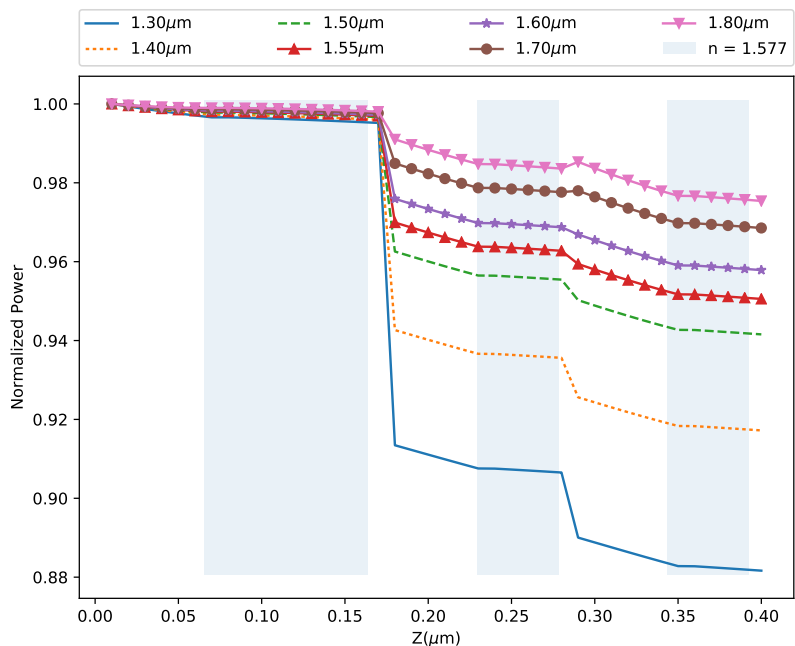

Fig. 9. H_y component normalized power for different wavelengths for the proposed SWG.

An interesting characteristic of this quasi-periodic segmented waveguide is that H_x component gains power along the propagation direction. The Fig. 10 shows this behaviour for different wavelengths.
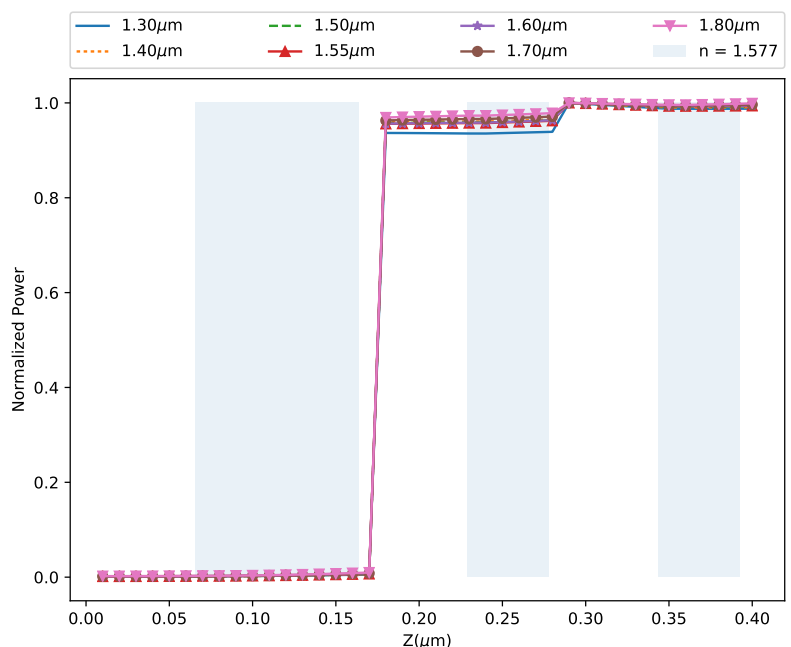

Fig. 10. H_x component normalized power for different wavelengths for the proposed SWG.

The Fig. 11 shown the normalized power, stored in the Hx and Hy fields along the propagation direction. The energy remains confined in the magnetic field polarized in the y direction, proving that

the sequence used in the stratification of the refractive indices in the guiding region, does not interfere in the initial polarization of the structure.
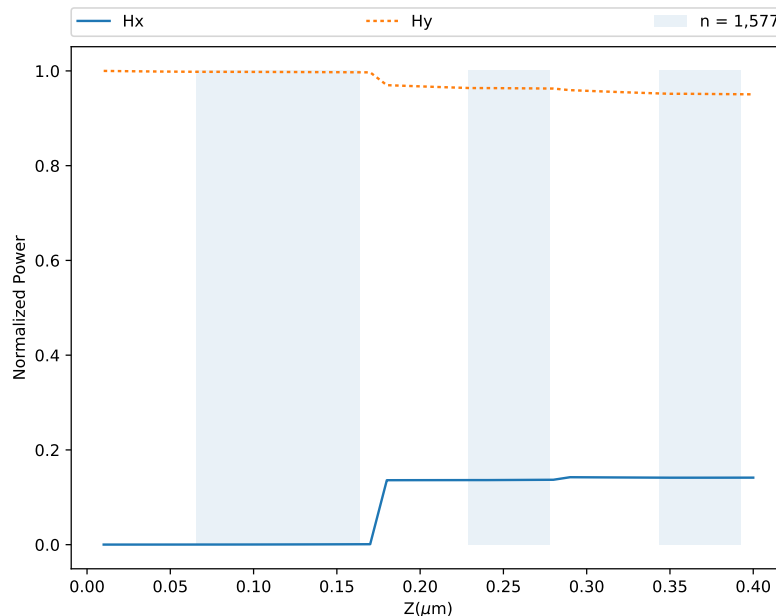

Fig. 11. Normalized power stored in the H_x and H_y fields along the propagation direction.

IV. CONCLUSIONS

In this work, a new type of structure based on a segmented waveguide, with sequential layers distributed in the guiding region and obtained from the Fibonacci sequence, was proposed. The structure combines a simple technology with a refractive index stratification in the guiding region distributed in a quasi-periodic formation. The propagation of the signal was theoretically analysed, from a mathematical formulation based on the vectorial beam propagation method in combination with the finite element method. The results obtained through numerical simulations show that the acquired performance corresponds to the distribution model of the layers with smaller losses for wavelengths ranging from $1.5 \mu m$ to $1.8 \mu m$, covering the optical bands of E, S, C, L and U.

ACKNOWLEDGMENTS

REFERENCES

[1] F. P. Payne and J. P. R. Lacey, "A theoretical analysis of scattering loss from planar optical waveguides," *Optical and Quantum Electronics*, vol. 26, no. 10, pp. 977–986, 1994.

[2] P. J. Bock, P. Cheben, J. H. Schmid, J. Lapointe, A. Delâge, S. Janz, G. C. Aers, D.-X. Xu, A. Densmore, and T. J. Hall, "Subwavelength grating periodic structures in silicon-on-insulator: a new type of microphotonic waveguide." *Optics express*, vol. 18, no. 19, pp. 20 251–62, 2010. [Online]. Available: http://www.osapublishing.org/viewmedia.cfm?uri=oe-18-19-20251{&}seq=0{&}html=true

[3] P. J. Bock, P. Cheben, J. H. Schmid, J. Lapointe, A. Delâge, D.-X. Xu, S. Janz, A. Densmore, and T. J. Hall, "Subwavelength grating crossing for silicon wire waveguides," *Optics Express*, vol. 18, no. 15, pp. 16 146–16 155, 2010.

[4] P. Cheben, P. J. Bock, J. H. Schmid, J. Lapointe, S. Janz, D.-X. Xu, A. Densmore, A. Delâge, B. Lamontagne, and T. J. Hall, "Refractive index engineering with subwavelength gratings for efficient microphotonic couplers and planar waveguide multiplexers," *Optics Express*, vol. 35, no. 15, pp. 2526–2528, 2010.

[5] C. E. Rubio-Mercedes, H. E. Hernández-Figueroa, J. Ivan T. Lima, and V. F. Rodríguez-Esquerre, "Periodic Segmented Waveguide Analysis by Using the 2D Finite Element Method," *IEE*, pp. 876–880, 2011.

[6] J. D. Joannopoulus, R. D. Meade, and J. N. Winn, "Photonics crystals: molding the flow of light," *Princeton University Press*, 1995.

[7] Z. Weissman, F. Saint-Andre, and A. Kevorkian, "Asymmetric directional coupler filters using buried ion-exchange, periodically segmented waveguides in glass." *Proc. ECIO'97*, p. 52, 2010.

[8] Z. Weissman, D. Nir, S. Ruschin, A. Hardy, S. Ruchin, and and A. Hardy, "Asymmetric Y-junction wavelength demultiplexer based on segmented waveguides," *Applied Physics Letters*, vol. 67, no. 3, pp. 302–304, 1995.

[9] J. Webjörn, F. Laurell, G. Arvidsson, J. Webjorn, F. Laurell, and G. Arvidsson, "Fabrication of periodically domain-inverted channel waveguides in lithium niobate for second harmonic generation," *Jornal of Ligthwave Technology*, vol. 7, no. 10, pp. 1597–1600, 1989.

[10] M. S. Gonçalves, Y. H. Isayama, and H. E. Hernández-Figueroa, "A novel three dimensional vector finite element method for periodic photonic devices," *Microwave and Optical Technology Letters*, vol. 58, no. 11, pp. 2665–2668, nov 2016. [Online]. Available: http://doi.wiley.com/10.1002/mop.30125

[11] H. Yun, Y. Wang, F. Zhang, Z. Lu, S. Lin, L. Chrostowski, and N. A. F. Jaeger, "Broadband 2 × 2 adiabatic 3 dB coupler using silicon-on-insulator sub-wavelength grating waveguides," *Optics Letters*, vol. 41, no. 13, p. 3041, 2016. [Online]. Available: https://www.osapublishing.org/abstract.cfm?URI=ol-41-13-3041

[12] R. Halir, P. Cheben, J. M. Luque-González, J. D. Sarmiento-Merenguel, J. H. Schmid, G. Wangüemert-Pérez, D. X. Xu, S. Wang, A. Ortega-Moñux, and Í. Molina-Fernández, "Ultra-broadband nanophotonic beamsplitter using an anisotropic sub-wavelength metamaterial," *Laser and Photonics Reviews*, vol. 10, no. 6, pp. 1039–1046, 2016.

[13] P. Cheben, D.-X. Xu, S. Janz, and A. Densmore, "Subwavelength waveguide grating for mode conversion and light coupling in integrated optics," *Optics Express*, vol. 14, no. 11, p. 4695, 2006. [Online]. Available: https://www.osapublishing.org/oe/abstract.cfm?uri=oe-14-11-4695

[14] D. Benedikovic, C. Alonso-Ramos, P. Cheben, J. H. Schmid, S. Wang, R. Halir, A. Ortega-Moñux, D.-X. Xu, L. Vivien, J. Lapointe, S. Janz, and M. Dado, "Single-etch subwavelength engineered fiber-chip grating couplers for 13 μm datacom wavelength band," *Optics Express*, vol. 24, no. 12, p. 12893, 2016. [Online]. Available: https://www.osapublishing.org/abstract.cfm?URI=oe-24-12-12893

[15] A. Sánchez-Postigo, J. Gonzalo Wangüemert-Pérez, J. M. Luque-González, Í. Molina-Fernández, P. Cheben, C. A. Alonso-Ramos, R. Halir, J. H. Schmid, and A. Ortega-Moñux, "Broadband fiber-chip zero-order surface grating coupler with 0.4 dB efficiency," *Optics Letters*, vol. 41, no. 13, p. 3013, 2016. [Online]. Available: https://www.osapublishing.org/abstract.cfm?URI=ol-41-13-3013

[16] P. Cheben, J. H. Schmid, S. Wang, D.-X. Xu, M. Vachon, S. Janz, J. Lapointe, Y. Painchaud, and M.-J. Picard, "Broadband polarization independent nanophotonic coupler for silicon waveguides with ultra-high efficiency," *Optics Express*, vol. 23, no. 17, p. 22553, 2015. [Online]. Available: https://www.osapublishing.org/abstract.cfm?URI=oe-23-17-22553

[17] D. Benedikovic, P. Cheben, J. H. Schmid, D.-X. Xu, B. Lamontagne, S. Wang, J. Lapointe, R. Halir, A. Ortega-Moñux, S. Janz, and M. Dado, "Subwavelength index engineered surface grating coupler with sub-decibel efficiency for 220-nm silicon-on-insulator waveguides," *Optics Express*, vol. 23, no. 17, p. 22628, 2015. [Online]. Available: https://www.osapublishing.org/abstract.cfm?URI=oe-23-17-22628

[18] D. Pérez-Galacho, D. Marris-Morini, A. Ortega-Moñux, J. G. Wangümert-Pérez, and L. Vivien, "Add/Drop Mode-Division Multiplexer Based on a Mach-Zehnder Interferometer and Periodic Waveguides," *IEEE Photonics Journal*, vol. 7, no. 4, 2015.

[19] J. Gonzalo Wangüemert-Pérez, P. Cheben, A. Ortega-Moñux, C. Alonso-Ramos, D. Pérez-Galacho, R. Halir, I. Molina-Fernández, D.-X. Xu, and J. H. Schmid, "Evanescent field waveguide sensing with subwavelength grating structures in silicon-on-insulator," *Optics Letters*, vol. 39, no. 15, p. 4442, 2014. [Online]. Available: http://ol.osa.org/abstract.cfm?URI=ol-39-15-4442{%}5Cnhttps://www.osapublishing.org/abstract.cfm?URI=ol-39-15-4442

[20] J. Flueckiger, S. Schmidt, V. Donzella, A. Sherwali, D. M. Ratner, L. Chrostowski, and K. C. Cheung, "Sub-wavelength grating for enhanced ring resonator biosensor," *Optics Express*, vol. 24, no. 14, p. 15672, 2016. [Online]. Available: https://www.osapublishing.org/abstract.cfm?URI=oe-24-14-15672

[21] Y. Xu and J. Xiao, "Ultracompact and high efficient silicon-based polarization splitter-rotator using a partially-etched subwavelength grating coupler," *Scientific Reports*, vol. 6, no. March, pp. 1–11, 2016. [Online]. Available: http://dx.doi.org/10.1038/srep27949

Brazilian Microwave and Optoelectronics Society-SBMO   received 26 Aug 2022; for review 15 Sept 2022; accepted 18 May 2023

Brazilian Society of Electromagnetism-SBMag   © 2023 SBMO/SBMag   (cc) BY   *ISSN 2179-1074*

[22] L. Liu, Q. Deng, and Z. Zhou, "Manipulation of beat length and wavelength dependence of a polarization beam splitter using a subwavelength grating," *Optics Letters*, vol. 41, no. 21, p. 5126, 2016. [Online]. Available: https://www.osapublishing.org/abstract.cfm?URI=ol-41-21-5126

[23] Y. Xiong, J. G. Wangüemert-Pérez, D.-X. Xu, J. H. Schmid, P. Cheben, and W. N. Ye, "Polarization splitter and rotator with subwavelength grating for enhanced fabrication tolerance," *Optics Letters*, vol. 39, no. 24, p. 6931, 2014. [Online]. Available: https://www.osapublishing.org/abstract.cfm?URI=ol-39-24-6931

[24] J. Wang, R. Ashrafi, R. Adams, I. Glesk, I. Gasulla, J. Capmany, and L. R. Chen, "Subwavelength grating enabled on-chip ultra-compact optical true time delay line," *Scientific Reports*, vol. 6, pp. 1–10, 2016. [Online]. Available: http://dx.doi.org/10.1038/srep30235

[25] J. S. Penades, A. Ortega-Moñux, M. Nedeljkovic, J. G. Wangüemert-Pérez, R. Halir, A. Z. Khokhar, C. Alonso-Ramos, Z. Qu, I. Molina-Fernández, P. Cheben, and G. Z. Mashanovich, "Suspended silicon mid-infrared waveguide devices with subwavelength grating metamaterial cladding," *Optics Express*, vol. 24, no. 20, p. 22908, 2016. [Online]. Available: https://www.osapublishing.org/abstract.cfm?URI=oe-24-20-22908

[26] J. Čtyroký, J. Wangüemert-Pérez, P. Kwiecien, I. Richter, J. Litvik, J. Schmid, Í. Molina-Fernández, A. Ortega-Moñux, M. Dado, and P. Cheben, "Design of narrowband Bragg spectral filters in subwavelength grating metamaterial waveguides," *Optics Express*, vol. 26, no. 1, pp. 3041–3044, 2018.

[27] J. P. da Silva, "Simulação por Elementos Finitos da Propagação de Feixes Ópticos em Estruturas Fotônicas," Ph.D. dissertation, UNICAMP, Campinas, SP, 2003.

[28] G. R. Hadley, "Wide-angle beam propagation using Padé approximation method," *Optics Letters*, vol. 17, no. 10, pp. 1426–1428, 1992.

[29] J. P. Berenger, "A perfectly matched layer for the absortion of electromagnetic waves," *Journal of Computational Physics*, vol. 114, no. 10, pp. 185–200, 1994. [Online]. Available: http://portal.acm.org/citation.cfm?id=195266

[30] M. Koshiba, Y. Tsuji, and M. Hikari, "Finite-element beam-propagation method with perfectly matched layers boundary conditions," *IEEE Transactions on Magnetics*, vol. 35, no. 3, pp. 1482–1485, 1999.